Performance of Asynchronous Time-Spreading and Spectrally Coded OCDMA Systems

Sang-Gyu Park, *Member, IEEE*, and Andrew M. Weiner, *Fellow, IEEE, Fellow, OSA*

***Abstract*—The performance of asynchronous coherent time-spreading optical code-division multiple-access (OCDMA) systems is evaluated semi-analytically and the results are compared with those of spectral coding OCDMA systems using ultrashort pulses. The fundamental multi-access interference limited performances are predicted to be identical.**

***Index Terms*—Multiple access interference (MAI), optical CDMA, spectrally coded, time-spreading.**

I. Introduction

RECENTLY, optical code-division multiple-access (OCDMA) is receiving new attention in optical communications communities [1]–[5]. In OCDMA, multiple users share the communication media by using codes uniquely assigned to each user. Because of the overlap of the signals from multiple users in both time and frequency domains and of the square-law detection common in optical communication, the performance of an OCDMA system is usually limited by multiple access interference (MAI), which is caused by the beating between the signal components from different users.

OCDMA systems can be divided into coherent and incoherent ones, and it is well known that coherent systems produce better performance [6], [7]. The coherent OCDMA can be divided again into time-spread (TS) OCDMA and spectral-coded (SC) OCDMA. The performance of SC-OCDMA systems limited by MAI was analyzed rigorously by Salehi *et al.* [8]. The performance of TS-OCDMA systems has been analyzed by Wang *et al.* [9]. However, in the analysis of [9], signal-interference beating and interference-interference beating were approximated to be independent from each other. Furthermore, to our knowledge, no direct comparison between the performances of TS-OCDMA and SC-OCDMA has ever been reported.

In this paper, we present our analytical analysis of bit-error-rate (BER) performance of asynchronous TS-OCDMA systems, which fully accounts for the correlation between beating terms and verify the validity of our model by Monte-Carlo (M-C) simulations. We show that the MAI-limited performance of TS-OCDMA is fundamentally identical to that of asynchronous SC-OCDMA systems. We then discuss practical differences between SC- and TS-OCDMA systems.

Manuscript received January 11, 2008; revised April 9, 2008. Current version published October 24, 2008.

S.-G. Park is with the Division of Electronics and Computer Engineering, Hanyang University, Seoul 133-791, Korea. He was with Purdue University, West Lafayette, IN 47906 USA on his sabbatical leave from Hanyang University. (e-mail: sanggyu@hanyang.ac.kr).

A. M. Weiner is with the School of Electrical and Computer Engineering, Purdue University, West Lafayette, IN 47907 USA (e-mail: amw@purdue.edu).

Color versions of one or more of the figures in this paper are available online at http://ieeexplore.ieee.org.

Digital Object Identifier 10.1109/JLT.2008.925054

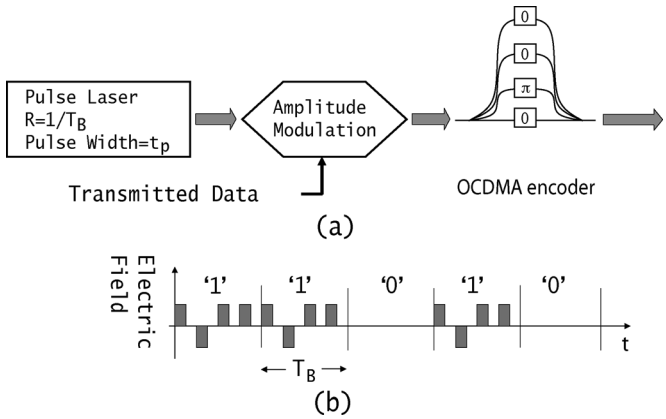

Fig. 1. (a) Schematic of TS-OCDMA transmitter. The OCDMA encoder is an interferometer with a phase modulator and delay in each arm. (b) Example of an output of OCDMA transmitter employing 4 chip OCDMA encoder, where the transmitted information sequence is "11010" and the OCDMA code sequence is "$+1-1+1+1$".

II. Analysis of TS-OCDMA Performance Under MAI

In this section, we analyze the BER performance of TS-OCDMA systems. Here, the assumptions on the system were setup as closely as possible to those of SC-OCDMA analysis of [8]. This will allow direct comparisons of TS- and SC-OCDMA performances.

A. System Description

Fig. 1(a) shows the schematic diagram of a TS-OCDMA transmitter used in this study. A transmitter has a short pulse laser with a pulse-width of $t_{\rm p}$ and the repetition rate of $1/T_{\rm B}$, where $T_{\rm B}$ is the bit period of the system. After binary amplitude-modulation by the transmitted information, the pulses enter an OCDMA encoder, which is an N_0-arm interferometer with a phase modulator in each arm as shown. The lengths of the arms of the interferometer are adjusted so that, for a single input pulse, we have a stream of N_0 pulses (or chips) separated by $T_{\rm C}$, which we call the chip period, at the output of the interferometer. Each of the N_0 pulses is binary phase modulated in the respective arm of the interferometer according to the OCDMA code uniquely assigned to each transmitter.

The performance of OCDMA systems depends on the OCDMA code. In this work, we use binary random codes, where for each OCDMA code sequence N_0 phases of either

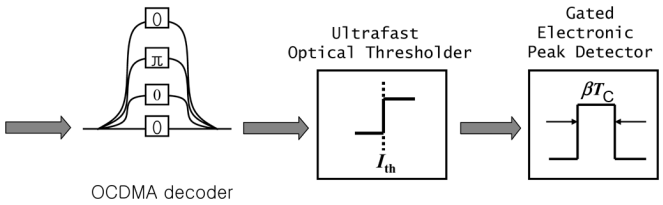

Fig. 2. Schematic of the TS-OCDMA receiver.

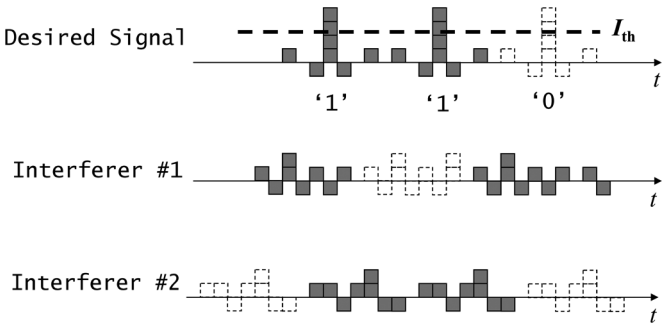

Fig. 3. Output fields from an optical correlator with a desired input and two interference signals.

0 and π are randomly chosen with equal probability $(= 1/2)$. We use random codes so that our results depend less on the properties of a particular code. Furthermore, the use of random code facilitates the comparison of our results with those in [8]. Fig. 1(b) shows an example of the OCDMA encoded optical signal from a transmitter, where $N_0 = 4$, $t_{\rm p} = T_{\rm C}/2$ and the OCDMA code sequence was $\{+1\ -1\ +1\ +1\}$.

The signals from multiple transmitters are then combined by a coupler and distributed to multiple receivers. Fig. 2 shows the schematic of the receiver. The received optical signal first goes into a correlator (OCDMA decoder), which is similar to the encoder. The phase and delay of each arm of the correlator are matched to that of the desired transmitter so that the correlation output from the desired signal has a strong autocorrelation (AC) peak. When the phases of encoder and decoder do not match as in the case of signals from interfering users, noise-like cross-correlation streams are obtained at the output. Fig. 3 illustrates the examples of the correlator output for the desired input and interference signals. The different starting point for each pulse stream indicates the asynchronous nature of the transmission.

The output of the correlator goes into an ultrafast optical thresholder, which generates "HIGH" output if the intensity of the signal into the thresholder is larger than a threshold and "LOW" output if not. In this study, an ideal thresholder which has infinite bandwidth and infinite output extinction ratio was assumed. Finally an electronic peak detector determines the received symbol by examining the presence of 'HIGH' in the output of the optical thresholder in a gating period $(T_G = \beta T_C)$. The gating period represents the temporal response time of electronic detector, which can be substantially longer than the chip-period $(\beta \gg 1)$ [8]. Note that a rectangular temporal response function is used to simplify the modeling.

In this work, it is assumed that there is no synchronism between the transmitters and that the synchronization between the desired transmitter/receiver pair has been established so that the receiver already knows the optimum sampling instance. Finally, it is assumed that the optical powers reaching a receiver from multiple transmitters are identical.

B. Performance Modeling

For the time being, we assume that $T_C = t_p$ and $T_B = 2N_0T_C$. With these conditions, the correlator output for a single bit completely fills a bit period as will be shown. These restrictions will be removed later. Also note that the above conditions correspond to a statistical multiplexing factor [8] $K = 2$, which we will define later.

We represent the received signal from the desired OCDMA transmitter transmitting a "1" symbol as a sum of rectangular pulses as

$$E_r(t) = \sqrt{P_d}\sum_{k=1}^{N_0} c(k)u(t/T_C - k) \tag{1}$$

where P_d is the peak power of the encoded signal, $c(k) = \{+1, -1\}$ is a binary OCDMA sequence, and $u(\ )$ is the unit square pulse function defined as

$$u(x) = \begin{cases} 1, & |x| < 1/2 \\ 0, & \text{otherwise} \end{cases}. \tag{2}$$

Because we are interested in the system performance limited by MAI and all the transmitters transmit an identical power, a particular choice of P_d does not affect the result. Therefore, we use $P_d = 1$ in the remaining of this paper to simplify the equations.

When the signal $E_r(t)$ enters into the correlator with the response of the arms given as $h(k)$, the output can be expressed as

$$\begin{aligned} E_{\rm dec}(t) &= \frac{1}{N_0}\sum_{j=1}^{N_0} E_r(t - jT_C)h(j) \\ &= \frac{1}{N_0}\sum_{k=1}^{2N_0-1} b(k)u(t/T_C - k) \end{aligned} \tag{3}$$

where

$$b(k) = \sum_{k=\max(1,k-N_0+1)}^{\min(k,N_0)} h(j)c(k-j+1) \tag{4}$$

is the correlation sequence between $h(k)$ and $c(k)$ and the factor of $1/N_0$ accounts for the intrinsic loss of the N_0 arm interferometer. Note that when a sequence of length N_0 is input to the correlator, the correlator produces an output sequence of length $2N_0 - 1$. The center element of the output sequence $(k = N_0)$ consists of contributions from all N_0 chips of the input, while the kth element from the center consists of contributions from $N_0 - |k|$ chips.

When the OCDMA code sequence of the desired transmitter is $c(k)$, the correlator response sequence is chosen as $h(k) =$

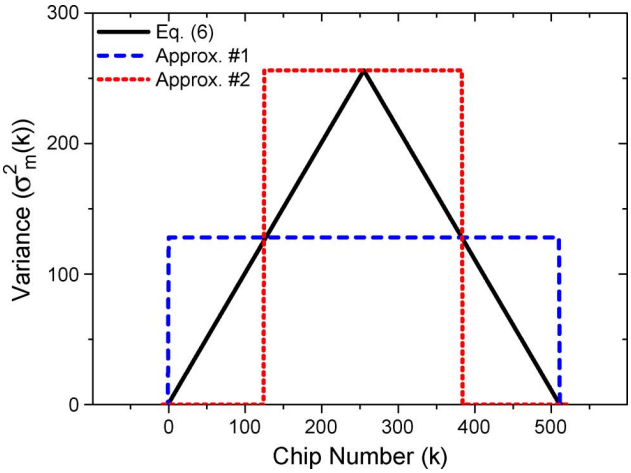

Fig. 4. Variance of $n_m(k)$ versus k : $N_0 = 256$.

$c(N_0 + 1 - k)$, so that we have an AC peak with magnitude of 1 (i.e., $\sqrt{P_d}$) at $k = N_0$. Note that this peak is to be detected by the combination of optical thresholder and electrical peak detector and that the gating period of the electrical peak detector is centered at $t = N_0 T_C$ (i.e., $k = N_0$).

Similarly, the cross-correlation output from a '1' symbol from the mth interference user transmitting such a symbol can be represented as

$$E_m(t) = \frac{1}{N_0} \sum_{k=1}^{2N_0-1} n_m(k) u(t/T_C - k - d_m) \exp(i\phi_m) \quad (5)$$

where $n_m(k)$ represents the random variable resulting from a convolution sum similar to (4) but with unmatched encoding and decoding sequences, and, ϕ_m and d_m represent the relative optical phase and delay between the desired signal and mth interference signal, respectively. For the sake of simplicity, we assume that the delay is an integer multiple of the chip period T_C.

To calculate the BER of the system, the distribution of $n_m(k)$ should be found. In general, it depends on the specific OCDMA code. In this work, as stated above, we use random codes. Then $n_m(k)$ becomes the sum of random binary sequence of $+1$ and -1 of length $N_0 - |N_0 - k|$ $(0 \le k \le 2N_0 - 1)$ and the distribution of $n_m(k)$ becomes binomial with zero mean and variance of [10]

$$\sigma_m^2(k) = N_0 - |N_0 - k| \quad (6)$$

which is shown as the solid line in Fig. 4. Note that $\sigma_m^2(k)$ does not depend on the particular interferer (m).

With the help of (5), the interference field from M_1 interference users transmitting '1' bits at $t = jT_C$ can be expressed as

$$E_{\text{inter}}(jT_C) = \frac{1}{N_0} \sum_{m=1}^{M_1} n_m(j - d_m) \exp(i\phi_m) = \frac{1}{N_0} \sum_{m=1}^{M_1} n_m(k_m) \exp(i\phi_m) \quad (7)$$

where $k_m \equiv j - d_m$. Because of the asynchronous nature of transmissions, k_m can be considered to be uniformly distributed between 0 and $2N_0 - 1$. Also note that the distribution of $E_{\text{inter}}(jT_C)$ is independent of j. Therefore, we drop j at this point.

To evaluate the BER of the system, we should obtain the distribution of E_{inter} and for that we represent E_{inter} as

$$E_{\text{inter}} = \alpha_x + i\alpha_y, \quad (8)$$

where α_x (or α_y) is a real random variable representing the real (or imaginary) part of E_{inter}.

With the help of central limit theorem, one can show that if M_1 is large and variances of $n_m(k)$ are $\sigma_m^2(k)$, then E_{inter} can be approximated to be a jointly Gaussian complex random variable, whose probability density function (pdf) can be represented as [11]

$$P(\alpha_x, \alpha_y | M_1) = \frac{1}{\pi \sigma_{M_1}^2} \exp\left(-\frac{\alpha_x^2 + \alpha_y^2}{\sigma_{M_1}^2}\right) \quad (9)$$

where

$$\sigma_{M_1}^2 = \sum_{m=1}^{M_1} \langle \sigma_m^2(k) \rangle / N_0^2. \quad (10)$$

The averaging $(\langle \cdot \rangle)$ in (10) is over k ranging from 0 to $2N_0 - 1$. This takes care of averaging over the different relative delays of the interfering users. If we substitute (6) in (10), we obtain

$$\sigma_{M_1}^2 = \frac{M_1}{2N_0}, \quad (11)$$

and (9) becomes

$$P_{\alpha_x \alpha_y}(\alpha_x, \alpha_y) = \frac{1}{\pi(M_1/2N_0)} \exp\left(-\frac{\alpha_x^2 + \alpha_y^2}{M_1/2N_0}\right). \quad (12)$$

This choice is equivalent to make $\sigma_m^2 = N_0/2$ independent of k as denoted as the dashed line (approx. #1) in Fig. 4.

However, in comparing to M-C simulations (see below), we have found that a much better match can be obtained when the distribution of variance is approximated by the dotted line (approx. #2) in Fig. 4. That is

$$\sigma_m^2(k) = \begin{cases} N_0, & |N_0 - k| < N_0/2 \\ 0, & \text{otherwise} \end{cases}. \quad (13)$$

This means that even though the length of the decoded pulse completely fills a bit period ($T_B = 2N_0 T_C$ and $T_C = t_p$), it has to be treated as if it has only 50% of probability of overlapping with a given sampling instant in the bit period. If we use (13), the probability that m out of M_1 interfering signals are effectively overlapped at the instance can be calculated to be

$$P_m(m|M_1) = \binom{M_1}{m} \left(\frac{1}{2}\right)^{M_1}. \quad (14)$$

Now, the pdf of the interference field can be represented by

$$P_{\alpha_x \alpha_y}(\alpha_x, \alpha_y) = \sum_{m=0}^{M_1} P_m(m|M_1) P_{\alpha_x \alpha_y}(\alpha_x, \alpha_y | m) \quad (15)$$

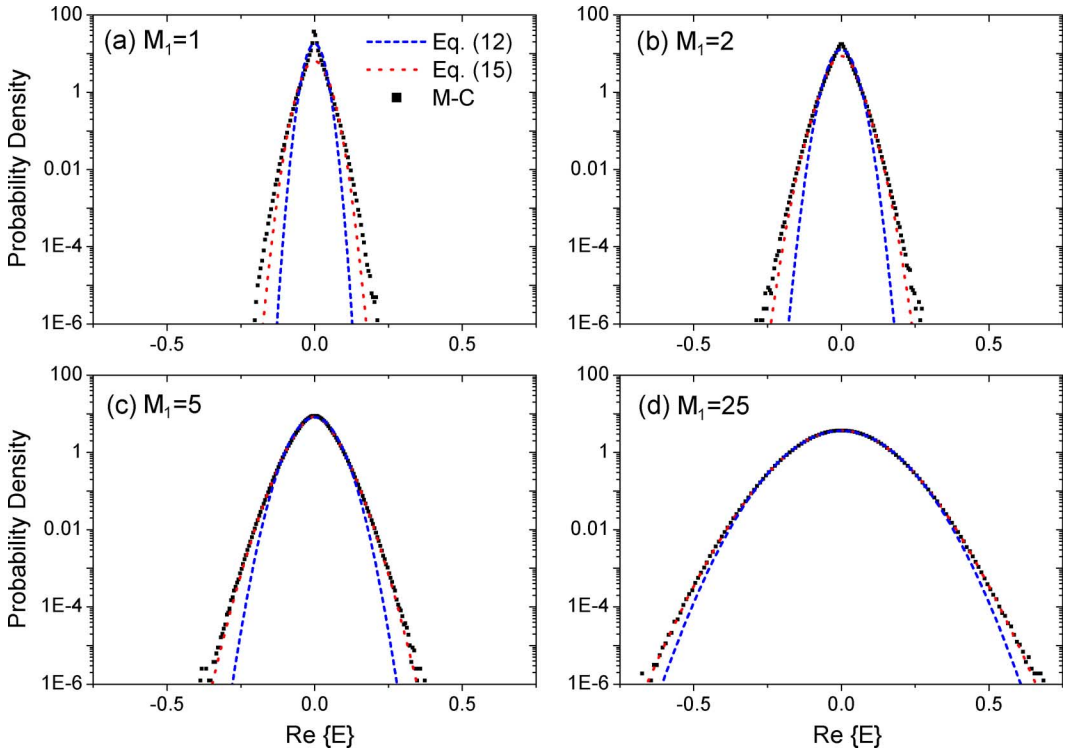

Fig. 5. Comparison of the pdfs for the field given by (7): $N_0 = 512$.

where

$$P_{\alpha_x\alpha_y}(\alpha_x, \alpha_y|m) = \frac{1}{\pi(m/N_0)} \exp\left(-\frac{\alpha_x^2 + \alpha_y^2}{m/N_0}\right) \quad (16)$$

is the Gaussian-approximated pdf of the interfering field conditioned on m effectively overlapped interfering signals.

Fig. 5 compares the pdfs of the real part of the electric field ($P_{\alpha_x}(\alpha_x) = \int P_{\alpha_x\alpha_y}(\alpha_x, \alpha_y)d\alpha_y$) obtained from (12) and (15) with the M-C simulation results. The details of the M-C simulation are presented in the next section. The symbols represent the results of M-C simulations and the dotted line represents (12), and the dashed line (15). We can observe that even for M_1 as small as 2, (15) produces a remarkable match to the M-C simulations, and for $M_1 \geq 5$ the match is almost perfect at least in the observed range. The match produced by (12) becomes gradually better as M_1 grows. However, even at $M_1 = 25$, (12) provides a reasonable fit only at the main body of the distribution, and in the tail region, which is very important for the accurate calculation of BER, (12) gradually departs from the M-C simulation results. We have performed M-C simulations with various M_1 and N_0 in the range relevant to our study ($1 \leq M_1 \leq 200$, $128 \leq N_0 \leq 1024$) and observed that (15) always provides a much better fit to M-C simulation than (12). Therefore, we choose the field distribution of (15) for our modeling.

Since the choice of the pdf of (15) is very important in this work, we compare (12) and (15) in more detail. When M_1 becomes very large, the pdf of (15) is dominated by the terms near $m = M_1/2$ because of the characteristics of the binomial distribution. Therefore, it is expected that the difference between the two pdfs diminishes as M_1 becomes large. This is confirmed in Fig. 6, which compares pdfs for $M_1 = 50$, 100, and 200. In Fig. 6(c), we can observe that the two pdfs cannot be distinguished. However, it should be noted that how large an M_1 is needed for the two pdfs to be practically identical depends on how low a probability level we wish to consider. If we look more closely at the tail of the distribution in Fig. 6(d), which is a expanded-range version of Fig. 6(c), we can again find slight disagreement between the pdfs.

With (15) as our model of the pdf of the interference field, we proceed to calculate the BER. For M active interfering transmitters, we can express the BER as

$$\mathrm{BER} = \sum_{m=0}^{M} P(m)\mathrm{BER}(m) \quad (17)$$

where $\mathrm{BER}(m)$ is the BER conditioned on m effective number of overlapped interfering correlation signals at the sampling instance and $P(m)$ is the probability of getting m effective interference signals. Furthermore, $P(m)$ can be expressed as

$$P(m) = \sum_{M_1=m}^{M} P_m(m|M_1)P_{M_1}(M_1|M), \quad (18)$$

where

$$P_{M_1}(M_1|M) = \binom{M}{M_1}\left(\frac{1}{2}\right)^M \quad (19)$$

represents the probability that M_1 out of M active transmitters are transmitting "1". Note that a transmitter transmits "1" or "0"

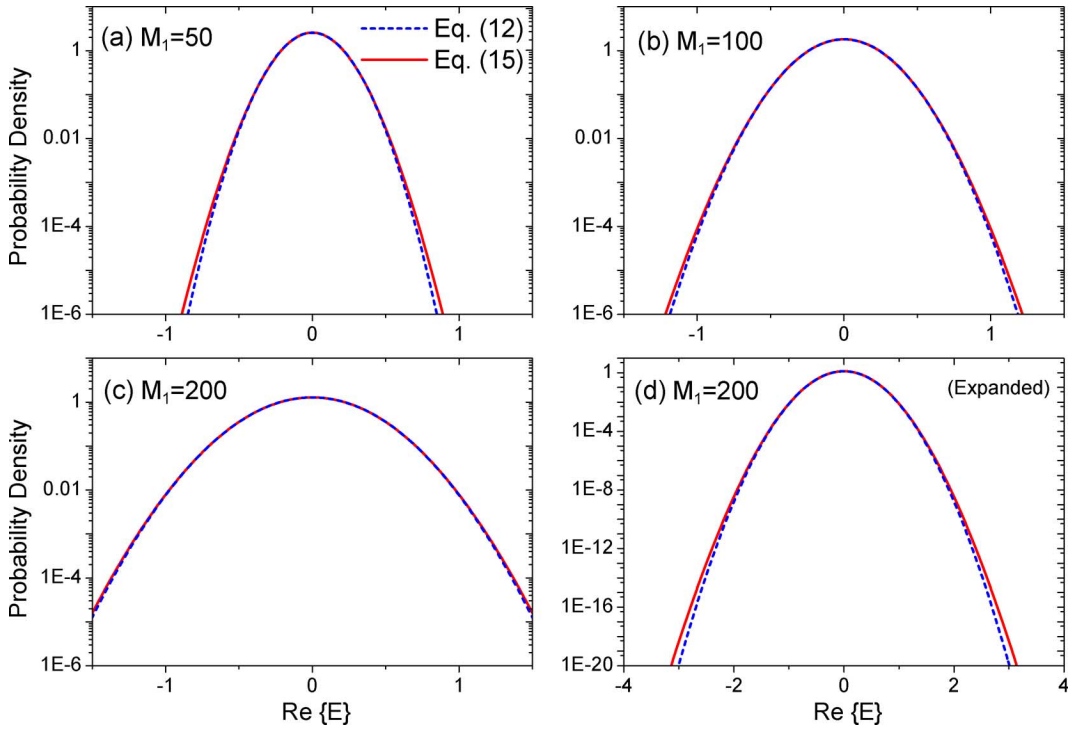

Fig. 6. Comparison of the pdfs: $N_0 = 512$.

with equal probabilities. $P_m(m|M_1)$ was defined in (14). After (14) and (19) are substituted into (18), it can be shown that

$$P(m) = \binom{M}{m}\left(\frac{1}{4}\right)^m\left(1-\frac{1}{4}\right)^{M-m}. \tag{20}$$

Eq. (20) can also be understood as a binomial distribution where $1/4 = (1/2)\cdot(1/2)$ comes from the 50% probability that a transmitter transmits "1"-bit AND the 50% probability (with the current set of parameters) that the correlator output from this "1"-bit is present at the instant of interest [see the discussion below (13)].

Now, it is straightforward to calculate BER following the line originally developed in [8]. For a given m, the pdf of the intensity of the thresholder input can be represented as

$$P_I(I|1,m) = \frac{1}{(m/N_0)}\exp\left(\frac{-I+1}{m/N_0}\right) I_0\left(\frac{\sqrt{I}}{m/2N_0}\right) \tag{21}$$

when the interference fields with the pdf of (15) is overlapped with an AC peak of a "1" bit transmitted from a desired user. In (21), $I_0(\cdot)$ is the modified Bessel function of the 0th order. When the interference field is not overlapped with the AC peak, the pdf becomes

$$P_I(I|0,m) = \frac{1}{(m/N_0)}\exp\left(-\frac{I}{m/N_0}\right). \tag{22}$$

Then, the probability of having a LOW output after the thresholder, despite the presence of the AC peak, can be expressed as

$$\rho(m) = \int_0^{I_{th}} p_I(I|1,m)dI. \tag{23}$$

Without an AC peak, the probability of a LOW output after the thresholder becomes

$$\gamma(m) = \int_0^{I_{th}} P_I(I|0,m)dI. \tag{24}$$

When a '0' bit is sent, an error occurs if a pulse is detected (i.e., the thresholder goes HIGH) in any of the β chip positions within the gating period of the electronic peak detector. This probability is

$$P_E(e|0,m) = 1-\gamma^{\beta}(m). \tag{25}$$

When a "1" bit is sent, an error occurs if no pulse is detected anywhere within the β chip positions (i.e., the thresholder never goes HIGH), and this probability is

$$P_E(e|1,m) = \rho(m)\gamma^{\beta-1}(m). \tag{26}$$

Finally, we can calculate BER(m) as

$$\mathrm{BER}(m) = \frac{1}{2}\left[1-\gamma^{\beta}(m)+\rho(m)\gamma^{\beta-1}(m)\right]. \tag{27}$$

This concludes the calculation of BER for $T_B = 2N_0T_C$ and $T_C = t_p$. The BER for other cases can be calculated by modifying the probability distribution of the effective number of overlapped signal given as (20). For this, we define the statistical multiplexing factor following [8]

$$K \equiv \frac{T_B}{N_0 t_p}. \tag{28}$$

Note that the case we have analyzed corresponds to $K = 2$. Following the same approach leading to (20), we can obtain

the following probability distribution of the effective number for $K \neq 2$.

$$P(m) = \binom{M}{m} \left(\frac{1}{2K}\right)^m \left(1 - \frac{1}{2K}\right)^{M-m}. \quad (29)$$

Other than this modification, the BER is given by (17) and ((21)–(27)) as before.

We can observe that the expressions for the performance of TS-OCDMA systems developed here are identical to those for the performance of SC-OCDMA systems in [8] [(42)–(45)]. The only difference is that here M is defined as the number of interference users, whereas in [8] it was defined as the total number of active users ($M_{\mathrm{Ref[8]}} = M + 1$). We present further discussion comparing TS- and SC-OCDMA, including M-C simulations confirming their identical MAI-limited performance, later in this paper.

C. Model Verification Through Monte-Carlo Simulations

In order to verify the validity of the analytical model, we performed Monte-Carlo (M-C) simulations of TS-OCDMA systems. In the simulations, while the signal from the desired user was fixed, the binary OCDMA code sequence, optical phases of individual pulses (φ_i) and delay of each interferer was randomly chosen for each iteration of M-C simulations. The delays were integral multiples of T_C. Because we used ideal rectangular pulses to represent the signal, we could use sequences of length N_0 to represent encoded signal or the response of the correlator, and could calculate $n_m(k)$ in (5) by a convolution sum between the correlator response and the encoded signal sequence. We repeated the simulations with various number of users, length of the OCDMA code, bandwidth of the electronic peak detector (β), and the statistical multiplexing factor (K). In our work, BERs were calculated down to 10^{-5}. It is very likely that OCDMA systems will operate with raw BERs larger than 10^{-5}. BERs lower than 10^{-15} can be obtained from such high raw BERs with the use of an error correcting code [12] while designing an asynchronous OCDMA system with a raw BER much lower than 10^{-5} will be very expensive, in terms of the required code length, as the results of this paper will indicate. The threshold of the optical thresholder was optimized for each number of active users.

Fig. 7 compares the results of analytic calculations and M-C simulations for several code-lengths (N_0). In all cases, $K = 1$ and $\beta = 1$ were used. We can observe very close agreement between the M-C simulations and the analytic modeling. We can also observe that as the code becomes longer, the BER performance is significantly improved. However, the use of longer codes requires shorter chip-period in addition to more complex encoder/decoders. A shorter chip-period, in turn, requires shorter optical pulses which are more difficult to generate and degrades spectral efficiency of the system. Furthermore, $\beta = 1$ means that the electronics operates at the chip rate, which will be nearly impossible with a large N_0.

In Fig. 8, we examine the performance of receivers with various electronic bandwidth parameters β, while keeping $N_0 = 1024$ and $K = 1$. Again, the agreement between the M-C simulations and analytic model is excellent. When β is increased from 1 to 1024, the number of users for $\mathrm{BER} = 10^{-5}$ decreases

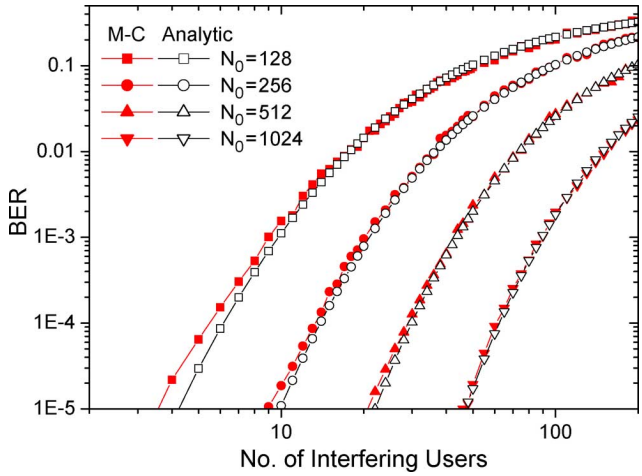

Fig. 7. Performance of TS-OCDMA systems with various code-lengths. $K = 1$, $\beta = 1$.

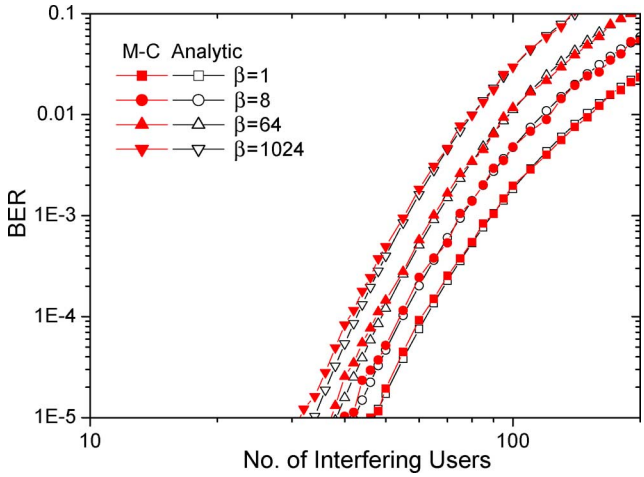

Fig. 8. Comparison of receivers with various electronic bandwidth parameter β. $N_0 = 1024$ and $K = 1$ for all cases.

from 48 to 34. Although the reduction of the number of user itself is significant, this might be acceptable for the more dramatic reduction of the bandwidth of the electronics. Note that $\beta = N_0 = 1024$ corresponds to the bit-rate electronics.

Fig. 9 compares the performance of OCDMA systems occupying the same optical bandwidth but using different code-lengths. Here we varied K and N_0 while fixing $N_0K = 1024$. In all cases $\beta = 1$ (chip-rate electronics) was used. Note that identical N_0K leads to identical chip period and optical bandwidth. Furthermore, when the chip period is identical, identical β leads to identical electrical bandwidth.

Besides an excellent match between the M-C simulations and analytic calculations, we can observe that the use of a longer code helps to improve the performance considerably when the number of users and the BER are relatively small. However, when the number of users and the BER are relatively large, systems with identical optical bandwidth have identical performance regardless of the combination of K and N_0. It means that when the pulse-width (chip-period) and bit-rate is fixed, increase of the code-length beyond a certain point does not improve the number of supported users.

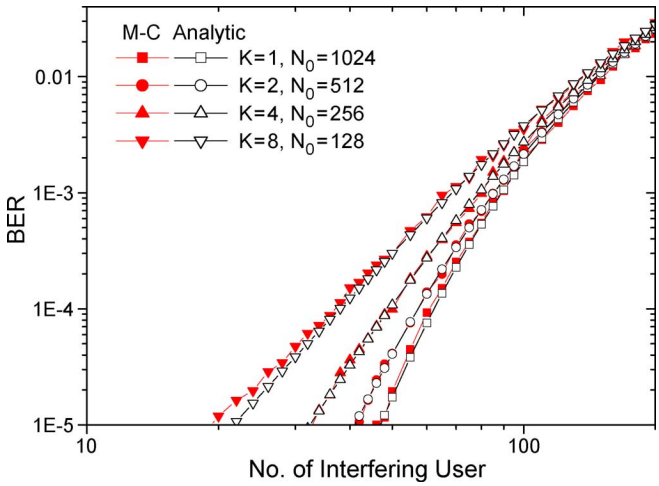

Fig. 9. Comparison of systems with identical optical bandwidth but with different K and code-length. $\beta = 1$.

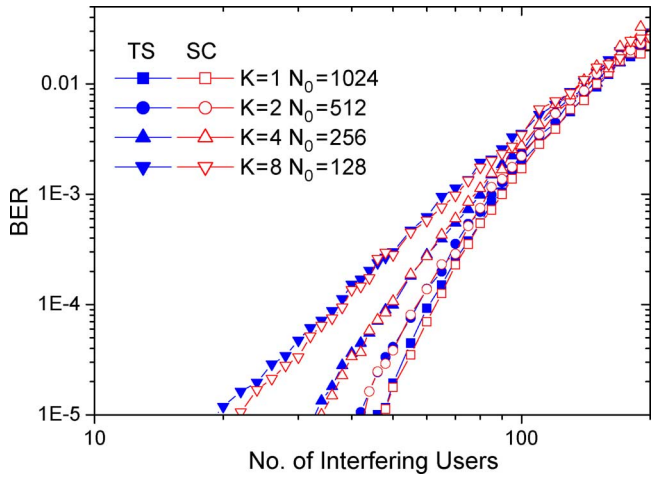

Fig. 10. Comparison of SC- and TS-OCDMA performances calculated by MC-simulations.

It should be noted that, in TS-OCDMA the statistical multiplexing can be realized in the following two methods or any combinations of them. In the first, the bit period is made longer than the encoded pulse sequence ($N_0 T_C < T_B$) but each chip period is completely filled with a pulse ($t_p = T_C$). In the second, a pulsewidth shorter than the chip-period is used, but the length of encoded pulse sequence is equal to the bit period. We performed M-C simulations using both methods and obtained identical results from them. (Data not shown.)

Finally, it was assumed in this work that the phase of the pulses were random. Even the phase of each pulse in a pulse stream from a single transmitter was varied randomly. When $K \geq 2$, the correlator outputs from neighboring pulses do not overlap, and this assumption should not cause any problem. Compared to the case of fixed-phase for all pulses in a pulse stream, it only affects the granularity of the error calculation (or the *burstiness* of errors.) Furthermore, our M-C simulation results show that even when the correlation output from neighboring pulses do overlap as in $K < 2$, the BER does not depend on the nature of the relative phase.

III. Comparison of Performance of TS- and SC-OCDMA Systems

As stated above, our theory predicts identical performance for TS-OCDMA and SC-OCDMA. To make a direct comparison, we performed M-C simulations of SC-OCDMA systems. As the encoded pulses were represented in the time domain by the sum of rectangular pulses for the TS-OCDMA, for SC-OCDMA, the encoded pulses were represented in the spectral domain by the sum of rectangles with equal magnitude whose phase is binary modulated according to the OCDMA code. Fig. 10 directly compares the performances of TS- and SC-OCDMA systems obtained by M-C simulations. We can observe a perfect match between the performances of them.

This equivalence between SC-OCDMA and TS-OCDMA may seem puzzling when we consider that TS-OCDMA loses some energy to correlation side-lobes while SC-OCDMA with phase only filters can concentrate 100% of the incoming signal at the sampling instance. This paradox can be explained if we consider the amplitude filtering of the correlators used in TS-OCDMA receivers.

We can see from (4) that the desired signal of a TS-OCDMA system produces optical power of 1 ($= P_d$) at the AC peak and the energy contained in that peak is $P_d t_p$. Next, from (6), we can calculate the average total optical energy contained in the correlation output from an interferer as

$$E_{XC} = \frac{\sum_{k=1}^{2N_0-1} (N_0 - |N_0 - k|)}{N_0^2} P_d t_p = P_d t_p \tag{30}$$

and the average power is given as $P_d t_p / T_B$. Therefore, the energy contained in the AC peak and the average total energy of the correlation output from an interferer is identical. Furthermore, it can be easily shown that the average energy contained in the side-lobes of the AC is almost identical to that in the cross-correlation.

Fig. 11 verifies the above results by comparing the power profiles of the output of the correlator from the desired and a interfering user. Fig. 11(a) shows the power profile from a single instance of M-C simulation and Fig. 11(b) shows the average over 1000 randomly chosen codes. In both cases, the interference signal was displaced by $192 T_C$ to facilitate the comparison. From Fig. 11(b), we can clearly observe that the profiles from the desired and the interference signals are identical except for the AC peak. Furthermore, from the average power in the side-lobes of $P_d/2N_0$, which is indicated by the dashed line, we can see that the total energy contained in a side-lobe is $2N_0 t_p P_d / 2N_0 = P_d t_p$, which is identical to the energy in the AC peak.

These results mean that even though the energies of pulse sequences incident on the correlator are identical, the average powers in the correlator output from the desired signal and the interferer differ by factor of 2 in average. This amplitude filtering which favors the desired signal over interferers is responsible for the identical performance of TS-OCDMA and SC-OCDMA despite the waste of energy in the AC side-lobes of TS-OCDMA.

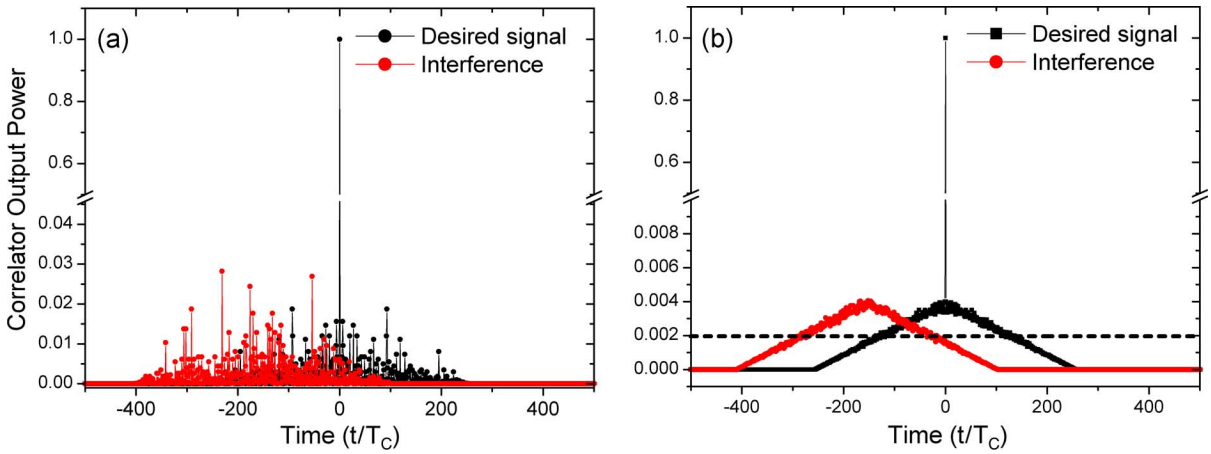

Fig. 11. Example of the output of the correlator. $N_0 = 256$ (a) Single instance. (b) Averaged over 1000 times with different OCDMA codes.

From the above discussion, it can be easily understood that the SNR of TS-OCDMA from a single interferer sending a "1" bit is

$$\mathrm{SNR_{TS}} = \frac{P_d}{P_d t_p / T_B} = \frac{T_B}{t_p}. \tag{31}$$

In SC-OCDMA with phase only filtering, all the power of both the desired signal and the interference reaches the optical thresholder after decoder. Then, because the power of the desired signal reaching the receiver is concentrated within t_p while the power of the power from an interferer is uniformly distributed over the period of T_B, the SNR of SC-ODMA from a single interferer is

$$\mathrm{SNR_{SC}} = \frac{T_B}{t_p} \tag{32}$$

which is identical to that of TS-OCDMA.

Actually, spectral amplitude filtering is also present to some degree in SC-OCDMA [13]. Unlike ideal phase only filtering, practical filters fundamentally exhibit some loss related to the transition of the phase between code chips. When the light passes through two filters with identical transition patterns, it loses less energy than when it passes two filters with different transition patterns. The tricky thing is that, even though the presence of this loss is fundamental, the amount of the loss is determined by the implementation details such as resolution of the optics. Because of this, it was not included in our performance comparison. However, as the number of chips is increased to the limit determined by the resolution of the optics, the filter loss is expected to play a significant role.

In this work, the focus was on the system performance limited by MAI and other sources of performance impairments such as receiver noise were not included. However, if the system performance is influenced by receiver noise, SC-OCDMA systems should have better performance because of the inherent loss associated with the optical correlators in TS-OCDMA systems. When there are N_0 branches in an optical correlator, only $2/N_0$ of the input power from the desired user shows up as the AC peak and AC side-lobes and the rest is lost in the correlator. This loss is fundamental and cannot be avoided. Therefore, when the effect of receiver noise cannot be ignored, it is expected that the performance of TS-OCDMA is worse than that of SC-OCDMA.

On the other hand, from the implementation point of view, it seems to be easier to obtain very large code-length in TS-OCDMA, for example using fiber Bragg gratings, than in SC-OCDMA systems. As we have seen, long code lengths are needed in order to obtain sufficient interference suppression if low BER (e.g., $< 10^{-9}$) is required in asynchronous OCDMA systems. Fully asynchronous operation of 10 user TS-OCDMA system with very low BERs has been reported at 1.25 Gb/s using 511-chip fiber Bragg grating encoder-decoders [3]. On the other hand, with the exception of an asynchronous two-user experiment performed at low bit rate [14], to our knowledge experimentation with SC-OCDMA systems has been limited to systems with at least some degree of timing coordination. This reflects relatively short code lengths (typically 31 to 63) and a focus on low raw BER. However, as revealed in Fig. 9, code length becomes much less important and statistical multiplexing becomes much more effective for systems operating at higher BER, e.g., 10^{-3}, in conjunction with FEC, provided that the bit rate—optical bandwidth product is held constant. Under such operation the practical code length advantage of TS-OCDMA will be less significant.

IV. Conclusion

In this paper, we calculated the BER performance of asynchronous, coherent TS-OCDMA and verified our calculations by M-C simulations. We also compared the performance of TS-OCDMA and SC-OCDMA systems and found that their fundamental MAI-limited performance is identical, while the considerations for receiver noise favor SC-OCDMA.

References

[1] J. P. Heritage and A. M. Weiner, "Advances in spectral optical code-division multiple-access communications," *IEEE J. Select. Topics Quantum Electron.*, vol. 13, no. 5, pp. 1351–1369, Sep.–Oct. 2007.

[2] X. Wang, N. Wada, T. Miyazaki, G. Cincotti, and K. Kitayama, "Asynchronous multiuser coherent OCDMA system with code-shift-keying and balanced detection," *IEEE J. Select. Topics Quantum Electron.*, vol. 13, no. 5, pp. 1463–1470, Sep.–Oct. 2007.

[3] T. Hamanaka, X. Wang, N. Wada, A. Nishiki, and K. Kitayama, "Ten-user truly asynchronous gigabit OCDMA transmission experiment with a 511-chip SSFBG En/decoder," *J. Lightw. Technol.*, vol. 24, no. 1, pp. 95–102, Jan. 2006.
[4] A. E. Willner, P. Saghari, and V. R. Arbab, "Advanced techniques to increase the number of users and bit rate in OCDMA networks," *IEEE J. Select. Topics Quantum Electron.*, vol. 13, no. 5, pp. 1403–1414, Sep.–Oct. 2007.
[5] A. M. Weiner, Z. Jiang, and D. E. Leaird, "Spectrally phase-coded O-CDMA," *J. Opt. Networking*, vol. 6, no. 6, pp. 728–755, 2007.
[6] D. D. Sampson and D. A. Jackson, "Coherent optical fiber communications system using all-optical correlation processing," *Opt. Lett.*, vol. 15, pp. 585–587, 1990.
[7] M. E. Marhic, "Coherent optical CDMA networks," *J. Lightwave Technol.*, vol. 11, no. 5/6, pp. 854–864, May–Jun. 1993.
[8] J. A. Salehi, A. M. Weiner, and J. P. Heritage, "Coherent ultrashort light pulse code-division multiple access communication systems," *J. Lightwave Technol.*, vol. 8, no. 3, pp. 478–491, Mar. 1990.
[9] X. Wang and K. Kitayama, "Analysis of beat noise in coherent and incoherent time-spreading OCDMA," *J. Lightwave Technol.*, vol. 22, no. 10, pp. 2226–2235, Oct. 2004.
[10] A. Papoulis, *Probability, Random Variables, and Stochastic Processes*, 3rd ed. New York: McGraw-Hill, 1991.
[11] J. W. Goodman, *Statistical Optics*. New York: Wiley, 1985.
[12] T. Mizuochi, "Recent progress in forward error correction and its interplay with transmission impairments," *IEEE J. Select. Topics Quantum Electron.*, vol. 12, no. 4, pp. 544–554, Jul.–Aug. 2006.
[13] Z. Jiang, D. S. Seo, D. E. Leaird, R. V. Roussev, C. Langrock, M. M. Fejer, and A. M. Weiner, "Reconfigurable all-optical code translation in spectrally phase-coded O-CDMA," *J. Lightwave Technol.*, vol. 23, no. 6, pp. 1979–1990, Jun. 2005.
[14] S. Shen, A. M. Weiner, and G. D. Sucha, "Bit error rate performance of ultrashort-pulse optical CDMA detection under multi-access interference," *Electron. Lett.*, vol. 36, pp. 1795–1797, 2000.

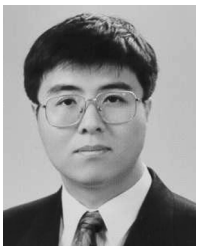

Sang-Gyu Park (S'88–M'99) received the B.S. and M.S. degrees in electronics engineering from Seoul National University, Seoul, Korea, in 1990 and 1992, respectively, and the Ph.D. degree in electrical and computer engineering from Purdue University, West Lafayette, IN, in 1998.

He was with AT&T Laboratories-Research from 1998 to 2000 and joined the faculty of Hanyang University, Seoul, in 2000, where he is an Associate Professor in Electronics and Computer Engineering. His research interests include optical transmission systems, optical CDMA networks, semiconductor devices, and circuits.

Andrew M. Weiner (S'84–M'84–SM'91–F'95) received the Sc.D. degree in electrical engineering from MIT, Cambridge, MA, in 1984.

He then joined Bellcore, first as a Member of Technical Staff and later as Manager of Ultrafast Optics and Optical Signal Processing Research. He moved to Purdue University, West Lafayette, IN, in 1992 and is currently the Scifres Distinguished Professor of Electrical and Computer Engineering. His research focuses on ultrafast optics signal processing and applications to high-speed optical communications and ultrawideband wireless. He is especially well known for his pioneering work in the field of femtosecond pulse shaping, which enables generation of nearly arbitrary ultrafast optical waveforms according to user specification. He has published six book chapters and over 200 journal articles. He has been author or co-author of over 350 conference papers, including approximately 80 conference invited talks, and has presented nearly 100 additional invited seminars at university, industry, and government organizations. He is holder of ten U.S. patents.

Dr. Weiner is a Fellow of the Optical Society of America (OSA) and a member of the National Academy of Engineering. He has won numerous awards for his research, including the Hertz Foundation Doctoral Thesis Prize (1984), the Adolph Lomb Medal of the Optical Society of America (1990), an award for pioneering contributions to the field of optics made before the age of 30, the Curtis McGraw Research Award of the American Society of Engineering Education (1997), the International Commission on Optics Prize (1997), the IEEE LEOS William Streifer Scientific Achievement Award (1999), the Alexander von Humboldt Foundation Research Award for Senior U.S. Scientists (2000), and the inaugural Research Excellence Award from the Schools of Engineering at Purdue (2003). He has served as Co-Chair of the Conference on Lasers and Electro-optics and the International Conference on Ultrafast Phenomena and as associate editor of several journals. He has also served as Secretary/Treasurer of IEEE LEOS and as a Vice-President of the International Commission on Optics (ICO).